Electronic Supplementary Material (ESI) for Journal of Materials Chemistry A.
This journal is © The Royal Society of Chemistry 2018

—Supporting Information—

Bioinspired Photothermal Conversion Coatings with Self-Healing Superhydrophobicity for Efficient Solar Steam Generation

Dehui Weng, Fuchang Xu, Xiang Li, Yang Li and Junqi Sun*

State Key Laboratory of Supramolecular Structure and Materials, College of Chemistry, Jilin University, Changchun 130012, PR China.

*E-mail: yanglichem@jlu.edu.cn

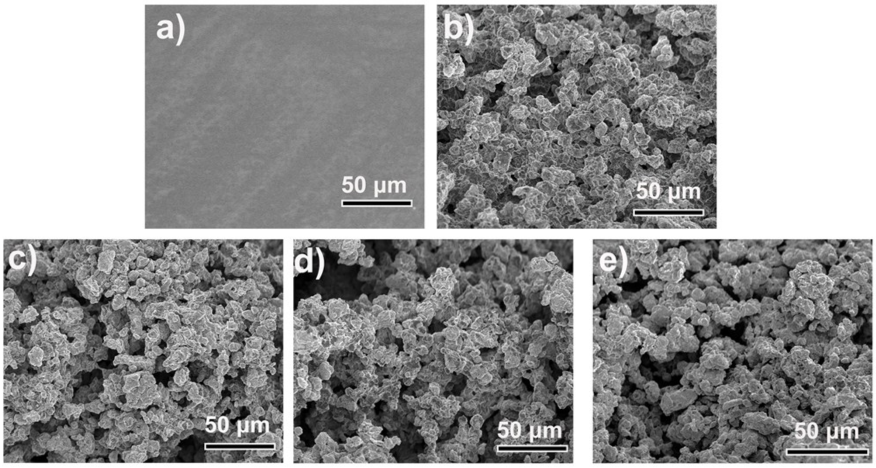

Fig. S1 SEM images of (a) the bare glass and the BCP_n coatings with n being (b) 1, (c) 3, (d) 5, and (e) 7.

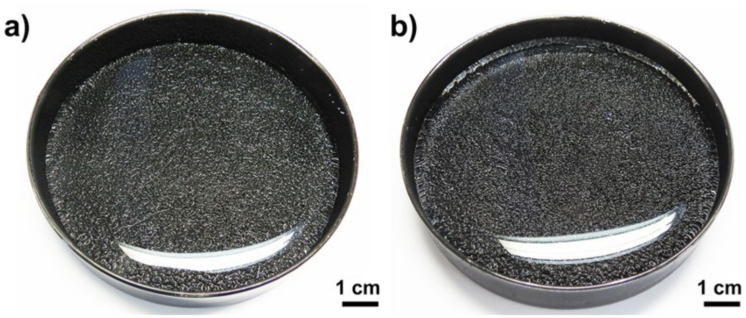

Fig. S2 (a) Photo image of the BCP_7-coated petri dish with 50 mL of water. (b) Photo image of the petri dish in (a) after being placed in ambient conditions for 2 months.

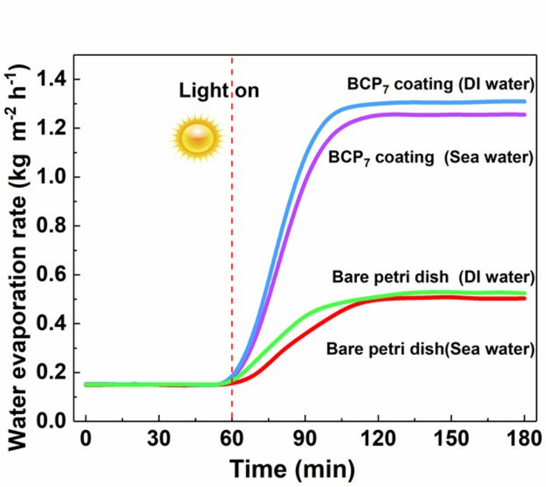

Fig. S3 Evaporation rates of the DI water and sea water in the BCP_7-coated and bare petri dishes under simulated solar light irradiation.

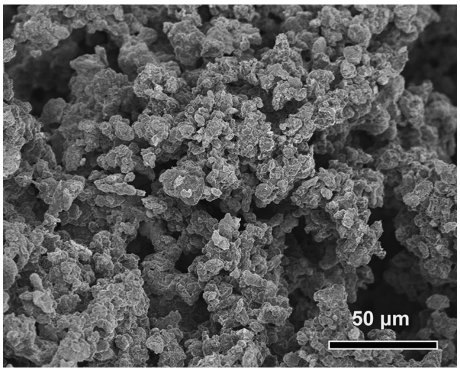

Fig. S4 SEM image of the BCP_7 coating that experienced a 56-h solar steam generation experiment.

After 56 h of solar steam generation (8 h a day for 7 d), no decomposition of the BCP_7 coating was observed. The CA and SA on the BCP_7 coating remained at 159.1° and 1.0°, respectively. The SEM image of the coating indicates that the surface structures of the coating was well preserved (Fig. S4).

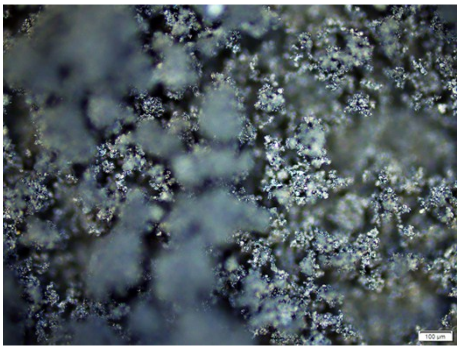

Fig. S5 Microscope image of the surface of the BCP_7 coating after evaporating sea water for 56 h.

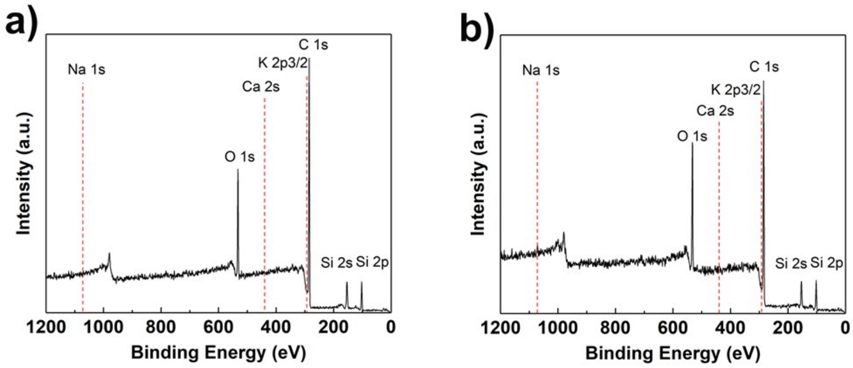

Fig. S6 XPS spectra of the BCP_7 coating (a) before and (b) after evaporating sea water for 56 h.

As shown in Fig. S6b, the signals for Na, Ca and K were not found, suggesting that the salt accumulation on the BCP_7 coating was negligible.

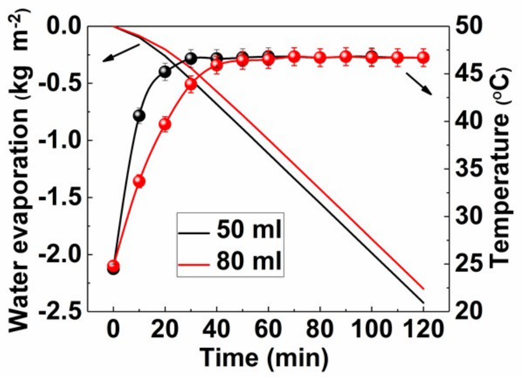

Fig. S7 Changes of the temperature and mass of 50-mL and 80-mL water under light irradiation.

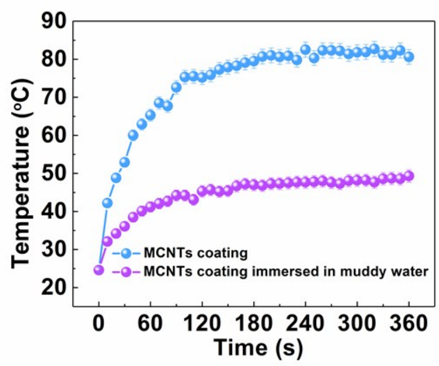

Fig. S8 Photothermal conversion ability of the MCNTs coating before and after immersion in muddy water for 12 h.

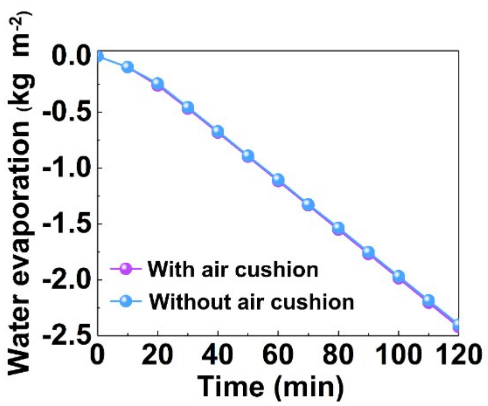

Fig. S9 Changes of the water mass in the BCP_7-cotaed petri dish with and without air cushion.

Fig. S10 Optical image of the portable balance that was used to measure the mass loss of water in the BCP_7-coated petri dish under natural sunlight irradiation.

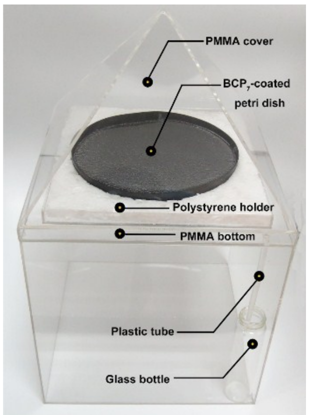

Fig. S11 Optical image of the portable solar desalination.

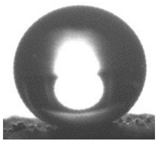

Fig. S12 CA on the BCP_7 coating after applying a voltage of 30 V for 30 min.

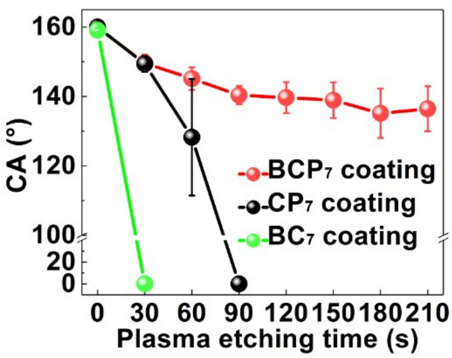

Fig. S13 CAs on the BCP_7, CP_7 and BC_7 coatings after plasma treatment for different time.

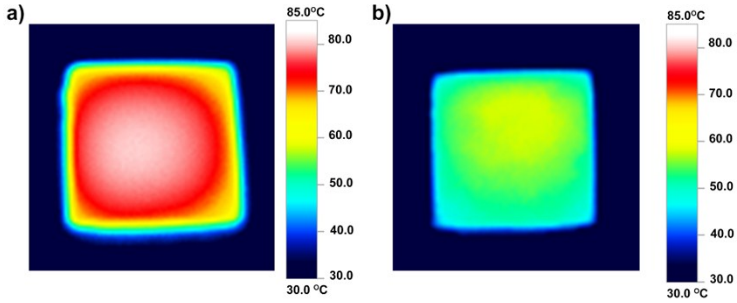

Fig. S14 Infrared images of photothermal abilities of (a) the BCP_7 coating experienced 20 etching/healing cycles and immersion in muddy water, and (b) the CP_7 coating experienced 5 etching/healing cycles and immersion in muddy water.

Table S1. Comparison of the self-healing ability, mechanical durability and conductivity of the BCP_7 coatings with different mass ratio of beeswax (b), MCNTs (c) and PDMS (p).

Mass Ratio (b:c:p)	Healing Cycles[a]	Sand Impact Test[b]	Conductivity (Ω sq^{-1})
0.5:2:1.5	4	Pass[c]	171.7 ± 7.9
1:2:1.5	20	Pass	232.3 ± 6.1
1.5:2:1.5	24	Fail[d]	1233.0 ± 82.8
1:2:1	21	Fail	215.9 ± 4.2
1:2:2	9	Pass	972.1 ± 42.6

a defined as the maximum number of plasma/healing cycles that the coating can repair its superhydrophobicity.

b sand grains with diameters ranging from 90 to 260 μm fell onto the sample, held at 45° to the horizontal surface, from a funnel with a drop rate of 12.85 g min^{-1}. The distance between the funnel and the sample was 2 m. Microscpoe images of the smaples are shown in Fig. S15.

c means that the surface structures of the coating was unchanged after being impinged by sands.

d means that the surface structures of the coating was damaged after being impinged by sands.

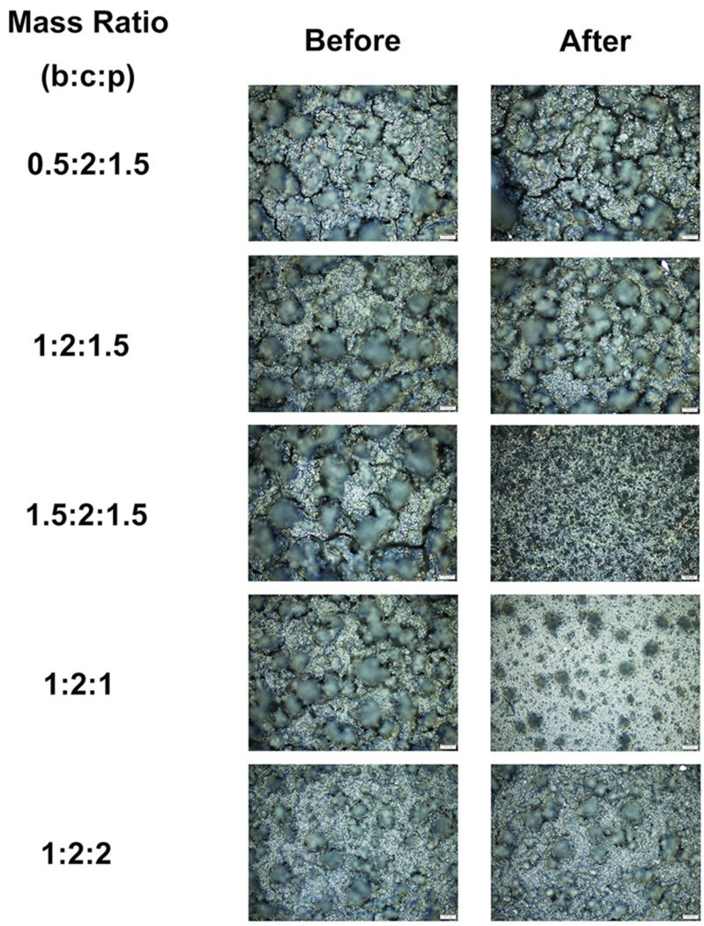

Fig. S15 Microscope images of surfaces the BCP_7 coatings with different mass ratio of beeswax, MCNTs and PDMS before (left column) and after (right column) sand impact experiments. The scale bars are 100 μm.